



Efficient Vacuum Deposited P-I-N Perovskite Solar Cells by Front Contact Optimization

Azin Babaei¹, Kassio P. S. Zanoni^{1*}, Lidón Gil-Escrig², Daniel Pérez-del-Rey¹, Pablo P. Boix¹, Michele Sessolo^{1*} and Henk J. Bolink¹

¹ Instituto de Ciencia Molecular, Universidad de Valencia, Paterna, Spain, ² Helmholtz-Zentrum Berlin für Materialien und Energie GmbH, Berlin, Germany

OPEN ACCESS

Edited by:

Silvia Colella,
University of Salento, Italy

Reviewed by:

Iván Mora-Seró,
University of Jaume I, Spain
Vincenzo Pecunia,
Soochow University, China

*Correspondence:

Kassio P. S. Zanoni
kassio.zanoni@uv.es
Michele Sessolo
michele.sessolo@uv.es

Specialty section:

This article was submitted to
Physical Chemistry and Chemical
Physics,
a section of the journal
Frontiers in Chemistry

Received: 11 November 2019

Accepted: 23 December 2019

Published: 17 January 2020

Citation:

Babaei A, Zanoni KPS, Gil-Escrig L, Pérez-del-Rey D, Boix PP, Sessolo M and Bolink HJ (2020) Efficient Vacuum Deposited P-I-N Perovskite Solar Cells by Front Contact Optimization. *Front. Chem.* 7:936. doi: 10.3389/fchem.2019.00936

Hole transport layers (HTLs) are of fundamental importance in perovskite solar cells (PSCs), as they must ensure an efficient and selective hole extraction, and ohmic charge transfer to the corresponding electrodes. In p-i-n solar cells, the ITO/HTL is usually not ohmic, and an additional interlayer such as MoO₃ is usually placed in between the two materials by vacuum sublimation. In this work, we evaluated the properties of the MoO₃/TaTm (TaTm is the HTL N₄,N₄,N₄'',N₄''-tetra([1,1'-biphenyl]-4-yl)-[1,1':4',1''-terphenyl]-4,4''-diamine) hole extraction interface by selectively annealing either MoO₃ (prior to the deposition of TaTm) or the bilayer MoO₃/TaTm (without pre-treatment on the MoO₃), at temperature ranging from 60 to 200°C. We then used these p-contacts for the fabrication of a large batch of fully vacuum deposited PSCs, using methylammonium lead iodide as the active layer. We show that annealing the MoO₃/TaTm bilayers at high temperature is crucial to obtain high rectification with low non-radiative recombination, due to an increase of the electrode work function and the formation of an ohmic interface with TaTm.

Keywords: perovskite solar cell, molybdenum oxide, vacuum-deposition, processing, hole transport layer

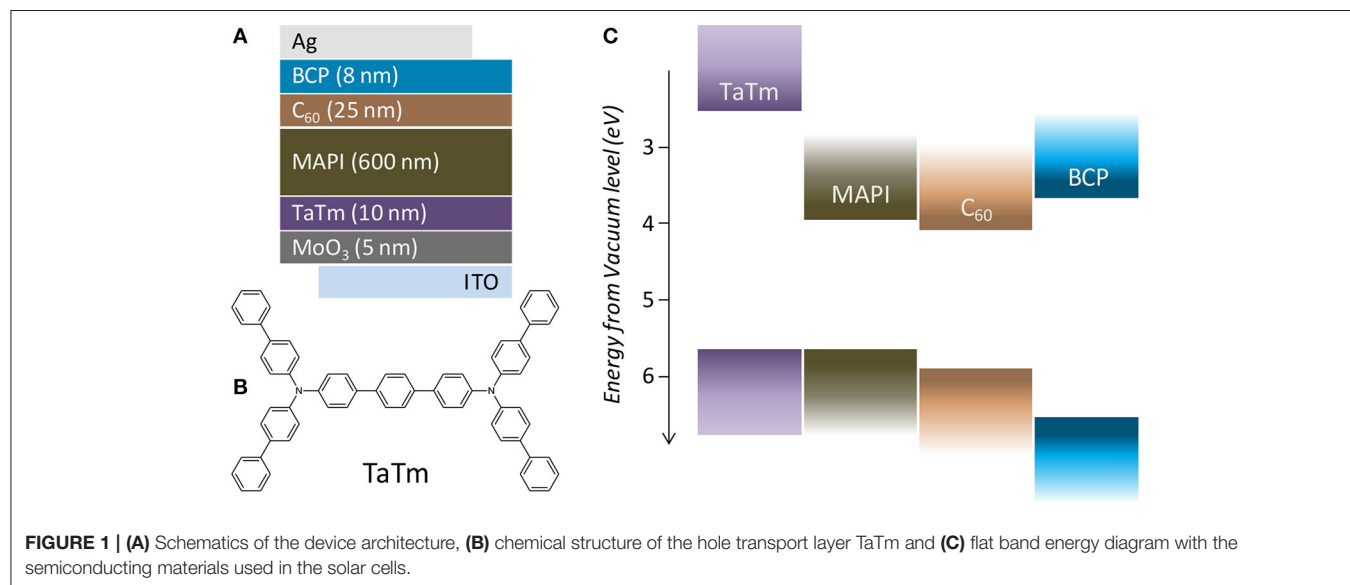
Perovskite solar cells (PSCs) are at the forefront of emerging photovoltaics materials, as demonstrated by the continuously rising power conversion efficiency (PCE) (Green et al., 2019). Achieving high conversion efficiencies requires placing the perovskite absorber in between selective charge transport layers that direct charge carriers to the appropriate electrodes for extraction (Pham et al., 2019; Shin et al., 2019). The choice of suitable charge selective materials depends on the type of device architecture used, the particular perovskite absorber, and on the thin-film processing technique. PSCs can be prepared in different architectures, depending on the polarity of the transparent electrode, normally a transparent conductive oxide (TCO) coated on a glass substrate. If the TCO front electrode is used as the p-contact, the structure is referred to as p-i-n, while if electrons are collected at the front contact, the solar cell is termed n-i-p. In p-i-n solar cells, the most common TCO is indium tin oxide (ITO), which is coated with a suitable hole transport layer (HTL) to selectively shuttle holes from the perovskite to the electrode. The hole transport material (HTM) should have a highest occupied molecular orbital (HOMO) or valence band close in energy to the perovskite valence band, as any mismatch would introduce losses in charge extraction or recombination (Schulz et al., 2015). Common molecular HTMs are arylamine derivatives (either polymers or isolated “small” molecules) and polythiophenes, due to their favorable hole mobility and suitable energy level alignment with most perovskite absorbers (Pham et al., 2019). While in some circumstances the direct ITO/HTL p-contact can lead to very

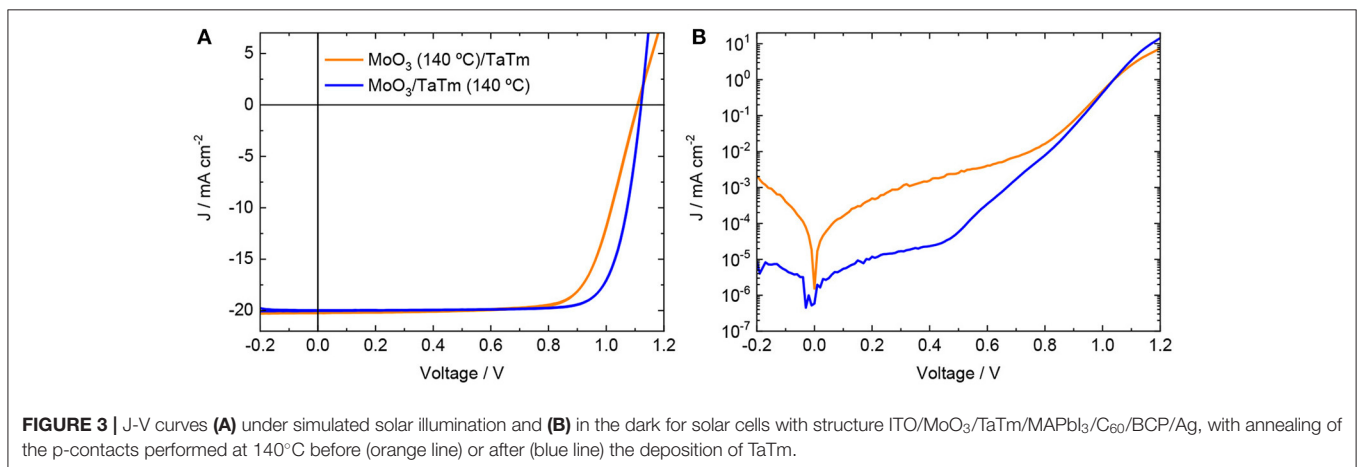
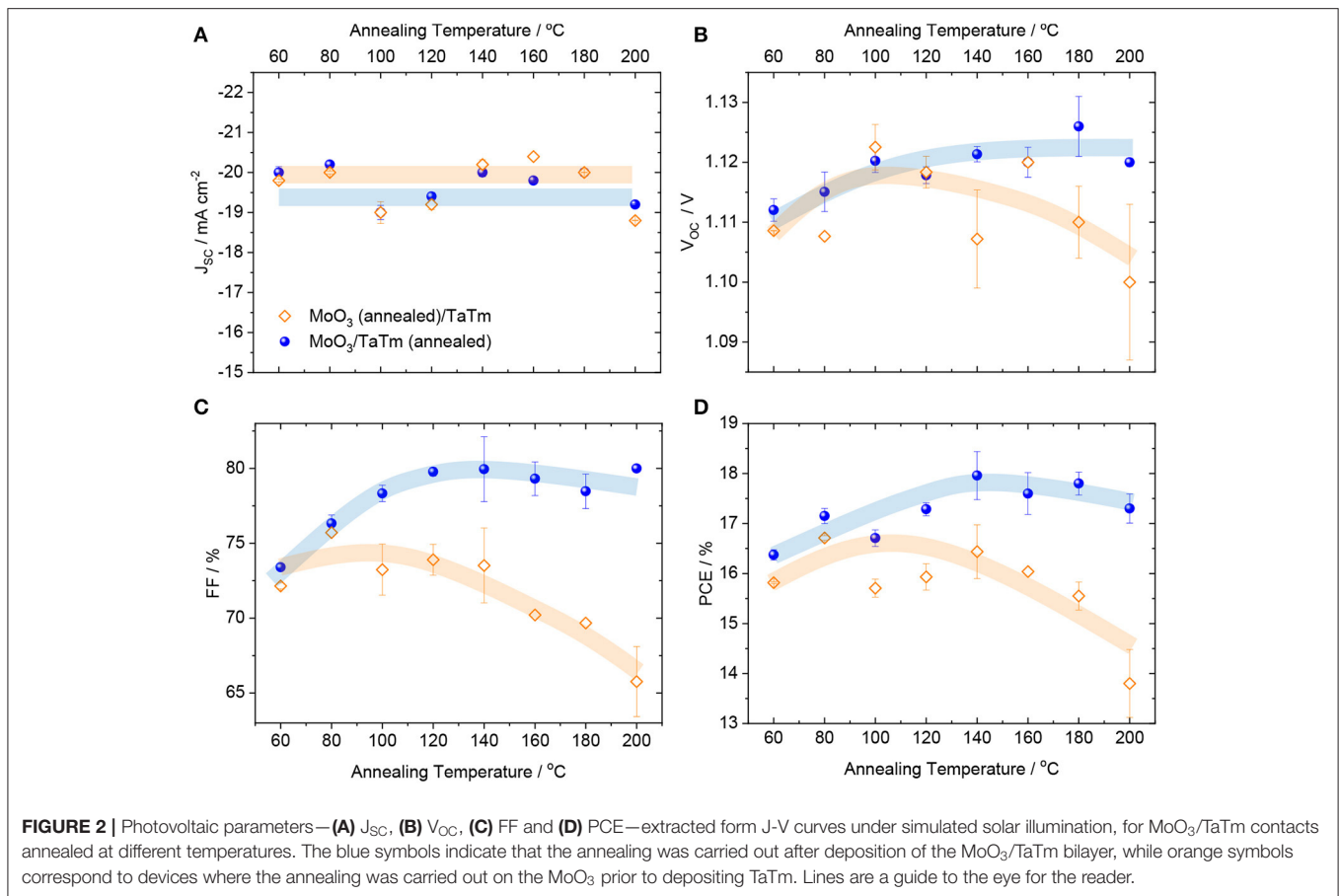
efficient charge collection (Al-Ashouri et al., 2019; Liu et al., 2019), the interface is not ohmic, and an additional interlayer is usually placed in between the ITO and the HTL (Schloemer et al., 2019). Common interface materials are high work function molecules (Avila et al., 2018), doped organic semiconductors (Momblona et al., 2016; Schloemer et al., 2019), or metal oxides such as MoO_3 , V_2O_5 , and W_2O_3 (Shin et al., 2019). MoO_3 is widely adopted as it can be deposited in thin-films by simple thermal vacuum sublimation, resulting in quasi-ohmic interfaces (Schulz et al., 2016). The use of vacuum deposition for transport layers and in particular for the perovskite gives several advantages over solution techniques. The thickness of each layer can be finely controlled, the materials purity is enhanced, and, more importantly, vacuum deposition methods are intrinsically additive, meaning that multilayer devices can be prepared without issues such as intermixing or partial redissolution of materials which are common to solution processing (Ávila et al., 2017). Recently, we have demonstrated the first vacuum-deposited PSCs with metal oxides at both the electron and the hole transporting layers (ETL and HTL) (Pérez-del-Rey et al., 2019). Both the p-i-n or n-i-p structures used MoO_3 at the p-contact, in combination with $\text{N}_4\text{N}_4\text{N}_4''\text{N}_4''$ -tetra([1,1'-biphenyl]-4-yl)-[1,1':4,1''-terphenyl]-4,4''-diamine (TaTm, **Figure 1**) as the HTM. In this work, we study the MoO_3 /TaTm interface and use post-deposition treatments in order to ensure an ohmic contact at the interface, demonstrating that a high work function MoO_3 is required to obtain high efficiency, vacuum deposited p-i-n PSCs.

For this study we used the following device configuration (**Figure 1**): ITO/ MoO_3 (5 nm)/TaTm (10 nm)/MAPI (600 nm)/ C_{60} (25 nm)/BCP (8 nm)/Ag (in which C_{60} is fullerene; BCP is bathocuproine and MAPI is methylammonium lead iodide). TaTm and C_{60} are intrinsic organic materials for charge selection, and MoO_3 and BCP are p- and n-contacts for efficient extraction of the photogenerated holes and electrons, respectively (Pérez-del-Rey et al., 2019; Zanoni et al., 2019). All

the layers in the device, including the MAPI perovskite film, were deposited by vacuum-assisted thermal evaporation, as described in the experimental section in the **Supporting Information**. To ensure sufficient statistics, for each device configuration, at least two different substrates each containing four cells were evaluated, while for top performing configurations at least five different substrates with a total of 20 cells were characterized. Due to the limited number of substrates (5) that can be processed in the setup used for these experiments, samples were fabricated through several perovskite deposition runs. Hence, small batch-to-batch variations might also contribute to the deviations observed in the photovoltaic parameters. We evaluated the properties of the MoO_3 /TaTm hole extraction interface by selectively annealing either MoO_3 (prior to the deposition of TaTm) or the bilayer MoO_3 /TaTm (without pre-treatment on the MoO_3), at temperature ranging from 60 to 200°C in a nitrogen atmosphere for 10 min. We then used these p-contacts for the fabrication of solar cells as described above. The series of devices was initially characterized under simulated solar illumination by measuring the current density vs. voltage (J-V) curves and extracting the relevant PV performance parameters (**Figure 2**).

As depicted in **Figure 2A**, all devices exhibited similar short-circuit current densities (J_{SC}) in the 19–20 mA cm^{-2} range, with small fluctuations originated from common batch-to-batch variability in the MAPI perovskite film properties. A difference in the temperature dependence can be observed for the open-circuit voltage (V_{oc} , **Figure 2B**), but especially for the fill factor (FF, **Figure 2C**). For both device series, we noted an increase in the photovoltage from 60 to $\sim 100^\circ\text{C}$, after which the V_{oc} was found to be high and stable (>1.12 V) for the cells with annealed MoO_3 /TaTm bilayer, or lower and progressively decreasing for the cells with annealed MoO_3 (until <1.11 V). The FF (**Figure 2C**) was found to steadily increase from 73% (at 60°C) to about 80% (in the 120–200°C range) for devices employing the annealed MoO_3 /TaTm bilayer. An opposite behavior was

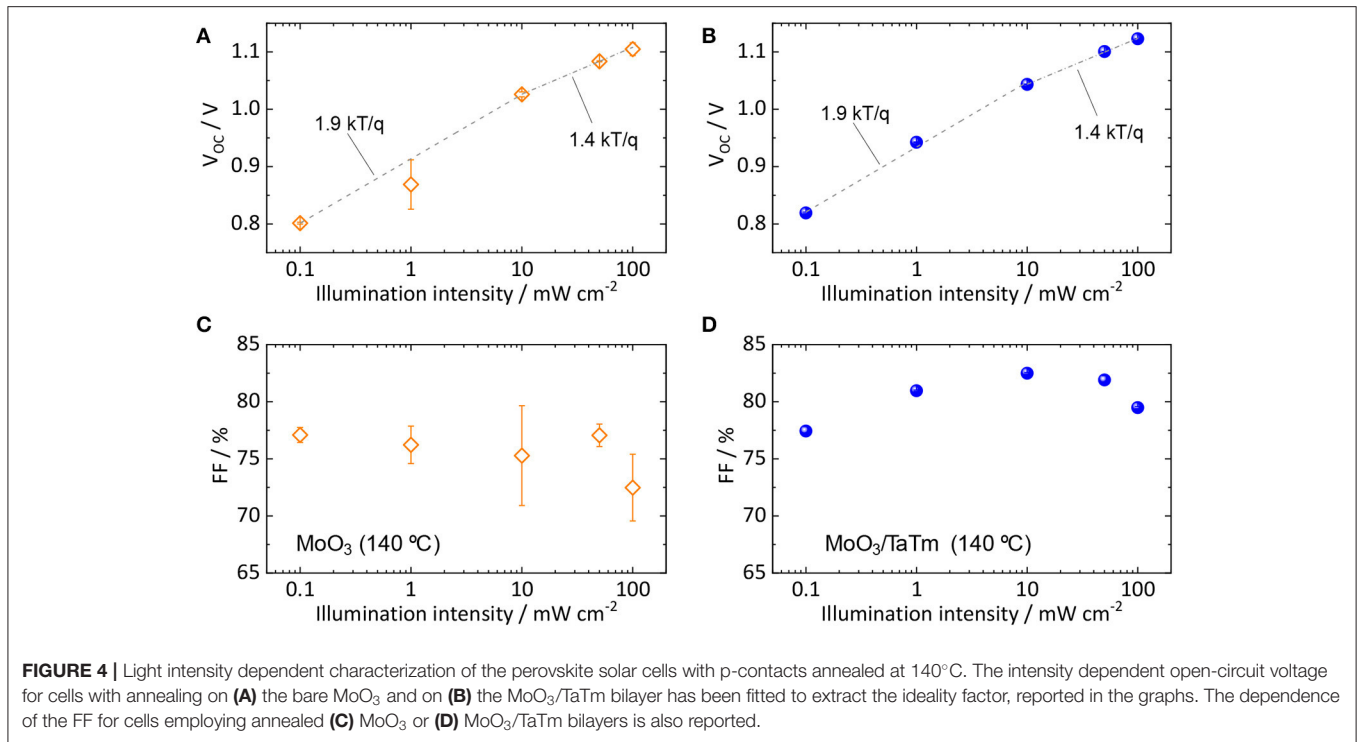




observed when annealing the MoO₃ prior to the deposition of TaTm. In this case the FF is rather constant at 72–73% until 140 °C, when it starts to progressively decrease reaching values of ~65% at 200 °C. The evolution of the V_{oc} and especially of the FF with the temperature determine the overall PCE. For solar cells with annealed MoO₃/TaTm bilayers, the PCE steadily increases from 60 °C (16.5%), reaching a maximum of 18% at 140 °C, and only slightly diminishing to still above 17% for higher

temperatures. On the other hand, the PCE of devices where annealing is carried out on the bare MoO₃ peaks at 140 °C (at 16.5%), but it is strongly limited at higher temperatures, with values below 14% for p-contact annealed at 200 °C.

The representative J-V curves under simulated solar illumination for the two types of device with p-contact annealed at 140 °C are reported in **Figure 3** (J-V curves for all the other investigated annealing temperatures are reported in **Figure S1**).



The device with a MoO₃ layer annealed before TaTm deposition exhibited fairly high V_{oc} of 1.105 V and J_{sc} of 20 mA cm⁻², but with a rather poor FF of 73%. This is caused by the reduced slope of the J-V curve after the maximum power point (>0.8 V), which reveals the presence of a high series resistance in these cells (hindered charge extraction/injection). The lower V_{oc} is likely related to the extraction issue, as charge accumulation at the interface can increase the probability of non-radiative recombination, as well as to the higher leakage current (J-V curves in dark, **Figure 3B**). On the contrary, having the TaTm top-layer deposited and annealed together with MoO₃ led to solar cells with high rectification (FF = 80%), meaning that charge carrier extraction and injection are enhanced. This can be clearly seen from the dark J-V curves, where the slope of the diffusion region (0.5–1 V) as well as the current density at 1.2 V outperform those of the other type of devices.

The same set of solar cells with the optimum annealing temperature (140°C) were also studied as function of the incident light intensity, as summarized in **Figure 4**. The V_{oc} dependence for both devices (**Figures 4A,B**) showed a higher slope at low light intensity, reduced when approaching 1 sun equivalent illumination (10–100 mW cm⁻²). Fitting the logarithmical dependence of the V_{oc} with the light intensity resulted in diode ideality factors (IF) of 1.9 and 1.4 for the low and high intensity regime, respectively. This behavior can be rationalized on the basis of a dominant trap-assisted recombination (IF = 2) in the bulk of the perovskite at low carrier concentration, and the appearance of surface recombination at the front contact (lowering the IF) which saturates the V_{oc} at higher light intensity (Tress et al., 2018). The trend

of intensity-dependent current density for the same devices (**Figure S2**) also suggest hindered charge extraction (increased recombination) at high light intensity, as the power factor α becomes < 1.

While no substantial differences could be discerned for the two set of devices, the V_{oc} was found to be systematically larger when annealing the TaTm on top of the MoO₃ buffer layer, indicating that non-radiative recombination is reduced with this p-contact.

The recombination processes and presence of traps can also be deduced from the trend of the FF with decreasing light-intensity. In a pure trap-assisted recombination regime, the FF decreases with decreasing light intensity as the trap density is constant while the carrier concentration diminishes. For free-carrier recombination, the FF would increase monotonically when decreasing the light intensity, as the recombination rate depends only on the charge densities (Sherkar et al., 2017). As can be seen from **Figure 4D** for the high efficiency device with annealed MoO₃/TaTm bilayer, free carrier recombination is present for light intensity above 10 mW cm⁻², while trap-assisted recombination dominates for low light intensities, in agreement with the trend of photovoltage (**Figure 4B**). On the other hand, the solar cells with the annealed MoO₃ did not show a clear trend in the intensity dependence of the FF, remaining rather low (<77%) at all charge carrier concentration. This might indicate the presence of an extraction barrier at the MoO₃/TaTm interface, which however does not lead to substantial recombination (as the intensity dependent V_{oc} is similar to the other devices). When the majority carriers (holes) are transferred from the perovskite into the TaTm, they can

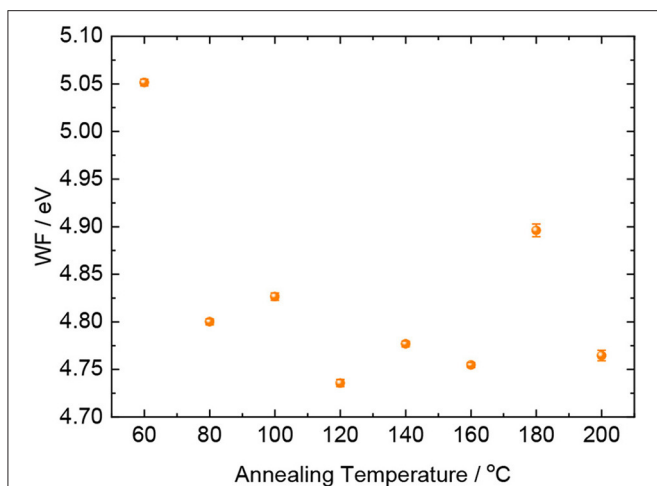


FIGURE 5 | Effect of annealing temperature on the WF of the surface of MoO₃ thin films deposited on ITO-coated glass slides.

recombine only with the minority carriers (electrons), leading to only small photovoltage losses. However, a potential barrier at the MoO₃/TaTm interface can still hinder their efficient collection at the front contact, reducing the FF of the solar cells. This barrier would also justify the series resistance observed for these diodes (Figure 3).

In order to shed light on the origin of this phenomena, we performed Kelvin probe measurements on the surface of MoO₃ as a function of the annealing temperature. We have to note that the experiments were performed in air, and hence the extracted work function (WF) values are affected by spontaneous adsorptions of atmospheric contaminants on the surface of MoO₃. We observed a WF = 5.05 eV for the sample annealed at 60°C, while for higher temperatures, the MoO₃ WF was found to decrease of ~0.2 eV (Figure 5). This WF reduction qualitatively agrees with the trend of the FF observed for cells with annealed solely on MoO₃, presented in Figure 2C. Hence the electrode WF might be held responsible for the extraction barrier and recombination at the front contact. The variation of the WF of MoO₃ with annealing is likely a consequence of increasing oxygen vacancies (Greiner et al., 2012), as in general reducing the oxidation state of any cationic center (such as by removal of oxygen) tends to decrease the metal oxide WF (Dasgupta et al., 2013). As Kelvin Probe is a surface sensitive technique, we could not extract meaningful information for the MoO₃ films coated with TaTm. In that case, the loss of oxygen upon annealing might be attenuated by the physical barrier

of TaTm itself, leading to a better ohmic contact within the MoO₃/TaTm interface (Pérez-del-Rey et al., 2019). Additionally, considering the high work function of MoO₃, hole transfer from the TaTm to MoO₃ is likely to occur (Xu et al., 2016), resulting in interfacial doping of TaTm and hence beneficial charge extraction.

In summary, the power conversion efficiencies of p-i-n PSCs can be modulated through the optimal processing of the MoO₃/TaTm HTLs. We observed that having the TaTm deposited and annealed together with the MoO₃ leads to large improvements in fill factor (>80%) and PCE (>18%) at any annealing temperature or light intensity, with the best results obtained for annealing at 140°C. These enhancements are accounted to an improved hole extraction rate and adjusted ohmic contact at the anode, which are likely due to an increased ITO/MoO₃ electrode work function.

DATA AVAILABILITY STATEMENT

The datasets generated for this study are available on request to the corresponding author.

AUTHOR CONTRIBUTIONS

AB, KZ, and LG-E fabricated and characterized the solar cells. DP-d-R and PB performed part of the characterization. MS and HB conceived the idea and directed the overall project. AB, KZ, and MS wrote the manuscript. All authors read and commented on the manuscript.

ACKNOWLEDGMENTS

Financial support is acknowledged from the Spanish Ministry of Economy and Competitiveness (MINECO) via the Unidad de Excelencia María de Maeztu MDM-2015-0538, MAT2017-88821-R, RTI2018-095362-A-I00, PCIN-2015-255, PCIN-2017-014, and the Generalitat Valenciana (Prome-teo/2016/135). KZ acknowledge the financial support from Fundação de Amparo à Pesquisa do Estado de São Paulo for financing a postdoctoral scholarship (2018/05152-7). MS thanks the MINECO for their RyC contracts.

SUPPLEMENTARY MATERIAL

The Supplementary Material for this article can be found online at: <https://www.frontiersin.org/articles/10.3389/fchem.2019.00936/full#Supplementary-Material>

REFERENCES

Al-Ashouri, A., Magomedov, A., Roß, M., Jošt, M., Talaikis, M., Chistiakova, G., et al. (2019). Conformal monolayer contacts with lossless interfaces for perovskite single junction and monolithic tandem solar cells. *Energy Environ. Sci.* 12, 3356–3369. doi: 10.1039/C9EE02268F

Avila, J., Gil-Escrig, L., Boix, P. P., Sessolo, M., Albrecht, S., and Bolink, H. J. (2018). Influence of doped charge transport layers on efficient perovskite solar cells. *Sustain. Energy Fuels* 2, 2429–2434. doi: 10.1039/C8SE00218E

Avila, J., Momblona, C., Boix, P. P., Sessolo, M., and Bolink, H. J. (2017). Vapor-deposited perovskites: the route to high-performance solar cell production? *Joule* 1, 431–442. doi: 10.1016/j.joule.2017.07.014

- Dasgupta, B., Goh, W. P., Ooi, Z. E., Wong, L. M., Jiang, C. Y., Ren, Y., et al. (2013). Enhanced extraction rates through gap states of molybdenum oxide anode buffer. *J. Phys. Chem. C* 117, 9206–9211. doi: 10.1021/jp3114013
- Green, M. A., Dunlop, E. D., Levi, D. H., Hohl-Ebinger, J., Yoshita, M., and Ho-Baillie, A. W. Y. (2019). Solar cell efficiency tables (version 54). *Prog. Photovoltaics Res. Appl.* 27, 565–575. doi: 10.1002/ppa.3171
- Greiner, M. T., Chai, L., Helander, M. G., Tang, W., and Lu, Z. (2012). Transition metal oxide work functions: the influence of cation oxidation state and oxygen vacancies. *Adv. Funct. Mater.* 22, 4557–4568. doi: 10.1002/adfm.201200615
- Liu, Z., Krückemeier, L., Krogmeier, B., Klingebiel, B., Márquez, J. A., Levchenko, S., et al. (2019). Open-circuit voltages exceeding 1.26 V in planar methylammonium lead iodide perovskite solar cells. *ACS Energy Lett.* 4, 110–117. doi: 10.1021/acsenergylett.8b01906
- Momblona, C., Gil-Escrig, L., Bandiello, E., Hutter, E. M., Sessolo, M., Lederer, K., et al. (2016). Efficient vacuum deposited p-i-n and n-i-p perovskite solar cells employing doped charge transport layers. *Energy Environ. Sci.* 9, 3456–3463. doi: 10.1039/C6EE02100J
- Pérez-del-Rey, D., Gil-Escrig, L., Zononi, K. P. S., Dreessen, C., Sessolo, M., Boix, P., et al. (2019). Molecular passivation of MoO₃: band alignment and protection of charge transport layers in vacuum-deposited perovskite solar cells. *Chem. Mater.* 31, 6945–6949. doi: 10.1021/acs.chemmater.9b01396
- Pham, H. D., Xianqiang, L., Li, W., Manzhos, S., Kyaw, A. K. K., and Sonar, P. (2019). Organic interfacial materials for perovskite-based optoelectronic devices. *Energy Environ. Sci.* 12, 1177–1209. doi: 10.1039/C8EE02744G
- Schloemer, T. H., Christians, J. A., Luther, J. M., and Sellinger, A. (2019). Doping strategies for small molecule organic hole-transport materials: impacts on perovskite solar cell performance and stability. *Chem. Sci.* 10, 1904–1935. doi: 10.1039/C8SC05284K
- Schulz, P., Tjepelt, J. O., Christians, J. A., Levine, I., Edri, E., Sanehira, E. M., et al. (2016). High-work-function molybdenum oxide hole extraction contacts in hybrid organic–inorganic perovskite solar cells. *ACS Appl. Mater. Interfaces* 8, 31491–31499. doi: 10.1021/acsmi.6b10898
- Schulz, P., Whittaker-Brooks, L. L., MacLeod, B. A., Olson, D. C., Loo, Y.-L., and Kahn, A. (2015). Electronic level alignment in inverted organometal perovskite solar cells. *Adv. Mater. Interfaces* 2:1400532. doi: 10.1002/admi.201400532
- Sherkar, T. S., Momblona, C., Gil-Escrig, L., Ávila, J., Sessolo, M., Bolink, H. J., et al. (2017). Recombination in perovskite solar cells: significance of grain boundaries, interface traps, and defect ions. *ACS Energy Lett.* 2, 1214–1222. doi: 10.1021/acsenergylett.7b00236
- Shin, S. S., Lee, S. J., and Seok, S. I. (2019). Metal oxide charge transport layers for efficient and stable perovskite solar cells. *Adv. Funct. Mater.* 29:1900455. doi: 10.1002/adfm.201900455
- Tress, W., Yavari, M., Domanski, K., Yadav, P., Niesen, B., Correa Baena, J. P., et al. (2018). Interpretation and evolution of open-circuit voltage, recombination, ideality factor and subgap defect states during reversible light-soaking and irreversible degradation of perovskite solar cells. *Energy Environ. Sci.* 11, 151–165. doi: 10.1039/C7EE02415K
- Xu, J., Voznyy, O., Comin, R., Gong, X., Walters, G., Liu, M., et al. (2016). Crosslinked remote-doped hole-extracting contacts enhance stability under accelerated lifetime testing in perovskite solar cells. *Adv. Mater.* 28, 2807–2815. doi: 10.1002/adma.201505630
- Zononi, K. P. S., Pérez-del-Rey, D., Dreessen, C., Angeles Hernández-Fenollosa, M., de Camargo, A. S. S., Sessolo, M., et al. (2019). Use of hydrogen molybdenum bronze in vacuum-deposited perovskite solar cells. *Energy Technol.* 1900734. doi: 10.1002/ente.201900734. [Epub ahead of print].

Conflict of Interest: The authors declare that the research was conducted in the absence of any commercial or financial relationships that could be construed as a potential conflict of interest.

Copyright © 2020 Babaei, Zononi, Gil-Escrig, Pérez-del-Rey, Boix, Sessolo and Bolink. This is an open-access article distributed under the terms of the Creative Commons Attribution License (CC BY). The use, distribution or reproduction in other forums is permitted, provided the original author(s) and the copyright owner(s) are credited and that the original publication in this journal is cited, in accordance with accepted academic practice. No use, distribution or reproduction is permitted which does not comply with these terms.